the cubane-type structure alkoxide oxygens are above the faces of the copper(II) tetrahedron and in the μ_4-oxo structure there is an oxygen at the center of the tetrahedron and a chloride above each edge; the close relationship between the bonding in these two types of structures has been discussed.[12]

Acknowledgments.—This work was supported by NSF Grant GP-7406. The help of the Rich Electronic Computer Center of Georgia Institute of Technology with computations is gratefully acknowledged.

(12) S. F. A. Kettle, *Theoret. Chim. Acta*, **4**, 150 (1966).

CONTRIBUTION NO. 1315 FROM THE CENTRAL RESEARCH DEPARTMENT, EXPERIMENTAL STATION, E. I. DU PONT DE NEMOURS AND COMPANY, WILMINGTON, DELAWARE 19898

The C Rare Earth Oxide–Corundum Transition and Crystal Chemistry of Oxides Having the Corundum Structure

BY C. T. PREWITT, R. D. SHANNON, D. B. ROGERS, AND A. W. SLEIGHT

Received December 2, 1968

Syntheses of new corundum-type phases at a pressure of 65 kbars show that complete solid solubility exists in the systems In_2O_3–Tl_2O_3, In_2O_3–Fe_2O_3, and Fe_2O_3–Ga_2O_3. Sc_2O_3 is soluble in In_2O_3 up to a ratio of about 1:1. A structure refinement of In_2O_3 II resulted in average interatomic distances essentially the same as those found for In_2O_3 I. Attempts to refine the structure of Tl_2O_3 II were not successful. Consideration of the structural relationships among corundum, B rare earth oxides, and C rare earth oxides and comparison of electronegativity differences between In_2O_3 and the rare earth oxides suggests why In_2O_3 and Tl_2O_3 transform to the corundum structure whereas Sc_2O_3, Y_2O_3, Lu_2O_3, and Tm_2O_3 transform to the B rare earth oxide structure at high pressure. Plots of effective cationic volume *vs.* unit cell volume, normalized c/a ratios *vs.* d-electron configuration, and metal–metal distances *vs.* effective ionic radii for all corundum-type phases provide a better understanding of the crystal chemistry of corundum-type oxides. Interatomic distances and c/a ratios are shown to be consistent with the Goodenough model which correlates electrical properties with metal–metal interactions. In addition, these correlations have been used to predict individual interatomic distances in the Rh_2O_3 structure.

Introduction

Several simple oxides are known to occur with the corundum (α-Al_2O_3) structure, including Al_2O_3, Ti_2O_3, V_2O_3, Cr_2O_3, Fe_2O_3, Ga_2O_3, and Rh_2O_3.[1] Recently, high-pressure transformations of In_2O_3 and Tl_2O_3, which normally have a C rare earth oxide structure, to a modification with the corundum structure[2] have been reported.[3,4] The corundum modification at high pressure was unexpected in that the usual high-pressure transformation observed for compositions with the C rare earth oxide structure is to the B rare earth oxide form. Hoekstra[5] found that even at intermediate pressures corundum structures are not formed for any of the rare earth oxides. Since density increases in the order C → corundum → B, it was not clear why the rare earth oxides are never found in a corundum modification, while In_2O_3 apparently never adopts the B form.[6] In order to attempt resolution of this problem, we have investigated the effects of pressure on the simple oxides Sc_2O_3, Y_2O_3, Lu_2O_3, Tm_2O_3, and Mn_2O_3 and on the ternary systems In_2O_3–Tl_2O_3, Fe_2O_3–Ga_2O_3, In_2O_3–Fe_2O_3, and In_2O_3–Sc_2O_3. We have also refined the structure of In_2O_3 II. Consideration of the results of this work in relation to the structures of the three available modifications provides a reasonable explanation for the high-pressure stabilization of the particular oxide phases in question.

Least-squares refinements of the structures of the following oxides have been reported: Al_2O_3,[7] Ti_2O_3,[7,8] V_2O_3,[7] Cr_2O_3,[7] Fe_2O_3,[7,9] Ga_2O_3,[10] and In_2O_3.[4] The availability of new crystallographic data for In_2O_3 II and Tl_2O_3 II, whose existence considerably broadens the stability field of known corundum phases, now provides a basis for considering the general crystal chemistry of corundum-type oxides. Such a consideration is also facilitated by the recent derivation of a set of ionic radii,[11] which appear to permit more reliable generalization. Accordingly, we present in the discussion of our work an attempt to correlate systematically the relations between observed structural parameters, chemistry of the various cations, ionic radii, and physical properties for the oxides that are known to have the corundum structure. Finally, the correlation of struc-

(1) R. W. G. Wyckoff, *Crystal Struct.*, **2**, 8 (1964).

(2) Throughout this paper, "corundum structure" will refer to any phase considered to be isotypic with α-Al_2O_3. The low-pressure forms (C rare earth or bixbyite structure) of In_2O_3 and Tl_2O_3 will be referred to as In_2O_3 I and Tl_2O_3 I. The high-pressure phases with the corundum structure will be referred to as In_2O_3 II and Tl_2O_3 II.

(3) R. D. Shannon, *Solid State Commun.*, **4**, 629 (1966).

(4) A. N. Christensen, N. C. Broch, O. V. Heidenstam, and A. Nilsson, *Acta Chem. Scand.*, **21**, 1064 (1967).

(5) H. R. Hoekstra, *Inorg. Chem.*, **5**, 754 (1966).

(6) In_2O_3, recently subjected to 120 kbars and 900°, still retains the corundum structure: A. F. Reid and A. E. Ringwood, *J. Geophys. Res.*, **74**, 3238 (1969).

(7) R. E. Newnham and Y. M. de Haan, *Z. Krist.*, **117**, 235 (1962).

(8) S. C. Abrahams, *Phys. Rev.*, **130**, 2230 (1963).

(9) R. L. Blake, R. E. Hessevick, T. Zoltai, and L. W. Finger, *Am. Mineralogist*, **51**, 123 (1966).

(10) M. Marezio and J. P. Remeika, *J. Chem. Phys.*, **46**, 1862 (1967).

(11) R. D. Shannon and C. T. Prewitt, *Acta Cryst.*, **B25**, 925 (1969).

TABLE I

CRYSTAL DATA FOR OXIDES HAVING THE CORUNDUM STRUCTURE

Compd	Effective ionic radius r, Å	r^3, Å^3	Cell dimensions, Å: a	c	c/a	Unit cell vol, Å^3	Electron confign	Electrical properties	Ref
Al_2O_3	0.53	0.149	4.759 ± 1	12.991 ± 5	2.73	254.80	$2p^6$	Insulator, $E > 8$ eV[f]	*a*
Cr_2O_3	0.615	0.233	4.961 ± 1	13.599 ± 5	2.74	289.85	$3d^3$		*a*
			4.954	13.584	2.74	288.72			*c*
Ga_2O_3	0.62	0.238	4.9825 ± 5	13.433 ± 1		288.80	$3d^{10}$	Insulator, $E = 4.8$ eV[f]	*b*
			4.9791 ± 6	13.437 ± 4	2.70	288.49			*e*
			4.9793	13.429		288.34			*c*
V_2O_3	0.64	0.262	4.952 ± 1	14.002 ± 5	2.83	297.36	$3d^2$	Semiconducting, metallic transition at ~150°K, $\rho_{RT} \cong 10^{-2}$ ohm cm[g]	*a*
Fe_2O_3	0.645	0.268	5.0345	13.749		301.80	$3d^5$	Insulator, $\rho_{RT} \cong 10^{13}$ ohm cm[g]	*a*
			5.0351 ± 3	13.750 ± 1	2.73	301.88			*e*
Rh_2O_3	0.665	0.294	5.108	13.81	2.70	312.05	$4d^6$		*d*
Ti_2O_3	0.67	0.301	5.149 ± 1	13.642 ± 8	2.63	313.23	$3d^1$	Semiconducting, metallic transition at 200°, $\rho_{RT} \cong 10^{-1}$ ohm cm[g]	*a, i*
			5.1572 ± 2	13.600 ± 1		313.26			*e*
In_2O_3 II	0.79	0.493	5.4870 ± 3	14.510 ± 1	2.64	378.33	$4d^{10}$	Semiconductor,[h] $E = 3.8$ eV	*e*
Tl_2O_3 II	0.88	0.681	5.7468 ± 3	14.851 ± 1	2.58	424.77	$5d^{10}$	Metallic?, $\rho_{RT} = 10^{-3}$ ohm cm[e]	*e*

[a] R. E. Newnham and Y. M. de Haan, *Z. Krist.*, **117**, 235 (1962). [b] M. Marezio and J. P. Remeika, *J. Chem. Phys.*, **46**, 1862 (1967). [c] H. E. Swanson, N. T. Gilfrich, and G. M. Ugrinic, "Standard X-Ray Diffraction Patterns," National Bureau of Standards Circular 539, U. S. Government Printing Office, Washington, D. C. [d] A. Wold, R. J. Arnott, and W. J. Croft, *Inorg. Chem.*, **2**, 972 (1963). [e] Data obtained in this work. Ti_2O_3 crystals were kindly supplied by P. Raccah and T. Reed, Lincoln Laboratories, M.I.T., Lexington, Mass. [f] H. H. Tippins, *Phys. Rev.*, **140A**, 316 (1965). [g] F. J. Morin, *Phys. Rev. Letters*, **3**, 34 (1959); F. J. Morin, *Bell System Tech. J.*, **37**, 1047 (1958). [h] R. L. Weiher and R. P. Ley, *J. Appl. Phys.*, **37**, 299 (1966). [i] S. C. Abrahams, *Phys. Rev.*, **130**, 2230 (1963).

tural parameters with effective ionic radii is used to predict interatomic distances in the unrefined Rh_2O_3 structure.

Experimental Section

Starting materials were oxides obtained from Spex Inc. and were of 99.999% purity except for Tl_2O_3 and Sc_2O_3 which were 99.99 and 99.9%, respectively. Ternary oxide mixtures were prepared by blending the oxides in alcohol, drying, and remixing dry. The process was repeated several times before pelleting the samples at 20,000 psi. These pellets were placed in cylindrical Pt holders, encased with a BN sleeve and covers, and placed inside a graphite sleeve, which served as a heater. This assembly was then placed in a pyrophyllite tetrahedron. The reactions were carried out in a tetrahedral anvil press whose operation and calibration were described by Bither, *et al.*[12] In all cases the samples were pressurized to either 65 or 89 kbars, heated to the reaction temperature, and allowed to react for 1 hr. The samples were quenched to room temperature in less than 60 sec by turning off the power. The pressure was then released slowly (3–4 min). The samples recovered from these runs were frequently composed of hexagonal prismatic crystals whose dimensions were approximately 0.2 × 0.5 mm.

X-Ray powder patterns were obtained at 25° on a de Wolff–Guinier camera; d values were calculated using λ(Cu $K\alpha_1$) 1.54051 Å with a KCl internal standard (a = 6.2931 Å). Table I lists cell dimensions obtained from a least-squares refinement of these data. Cell dimensions of Ga_2O_3, Fe_2O_3, and Ti_2O_3 were obtained in order to verify previously obtained literature values. The samples of Ga_2O_3 and Fe_2O_3 were prepared in highly crystalline form by heating at 65 kbars and 1100° for 1 hr. The sample of Ti_2O_3 was prepared by Reed, *et al.*[13] Chemical analysis of this sample indicated a stoichiometry of $TiO_{1.502}$. Cell dimensions of other samples of TiO_x where $x > 1.503$ show considerable variation from the values reported here. A structure refinement was carried out on crystals of In_2O_3 II and is reported below. Resistivity data were obtained by the four-probe method on single crystals of In_2O_3 II and $InScO_3$ II and on polycrystalline samples of Tl_2O_3 II, $TlInO_3$ II, and $InFeO_3$.

(12) T. A. Bither, J. L. Gillson, and H. S. Young, *Inorg. Chem.*, **5**, 1559 (1966).

(13) T. B. Reed, R. E. Fahey, and J. M. Honig, *Mater. Res. Bull.*, **2**, 561 (1967).

Synthesis and Properties of High-Pressure Corundum Phases

Table II lists some of the new corundum-phase products and their properties. Table III lists calculated and observed d values and observed intensities for In_2O_3 II and Tl_2O_3 II.

In_2O_3.—Hoekstra[5] found that In_2O_3 at pressures up to 60 kbars and temperatures of 550, 1000, and 1450° retained the C structure. Since the smaller rare earth (RE) oxides showed transitions to the B structure at high pressures, Hoekstra prediced a similar transition for In_2O_3.

Early experiments at 65 kbars and 1000° with mixtures of In_2O_3 and Co metal resulted in transparent brown crystals 0.05 mm in diameter. X-Ray powder patterns indicated the corundum structure (In_2O_3 II). Later experiments with pure In_2O_3 resulted in formation of II at temperatures as low as 800° if the sample had first been preheated to 1250°. If no preheating had occurred, formation of II took place only above 1000°. The presence of 2% Eu_2O_3 completely inhibited the transformation at 1200°.

Crystals of In_2O_3 II grown at temperatures from 800 to 1300° were transparent and colorless. Crystals grown above 1400° developed a deep blue color, which could be bleached by heating in air at 500° for several minutes. Presumably the blue color is caused by oxygen deficiency.

Crystals of In_2O_3 II approximately 0.5 mm in diam-

TABLE II
PROPERTIES OF NEW CORUNDUM PHASES

	Prepn temp, °C	a,[a] Å	c, Å	Cell vol, Å³	$\Delta V_{I \rightarrow II}/V_I$, %	ρ(25°), ohm cm; E,[b] eV
In_2O_3 II	800–1500	5.487	14.510	378.33	2.64	1.3×10^{-3} (single crystal)
Tl_2O_3 II	700–1000	5.747	14.851	424.77	3.42	10^{-3}; metallic? (polycrystal)
$GaFeO_3$ II	1200	5.023		297.53	5.07	
$InScO_3$ II	1250	5.404	13.615 14.412	364.45	2.08	4×10^{9}; 0.72 (single crystal)
$TlInO_3$ II	800	5.608	14.637	398.72	3.7	3.2×10^{-3}; metallic (polycrystal)
$InFeO_3$	1200	5.279	14.120	340.81		4; 0.08 (polycrystal)

[a] Calculated errors for all cell dimensions were less than 1 part in 10^4. [b] Derived from the slope of log ρ *vs.* $1/T$.

TABLE III
POWDER DIFFRACTION DATA FOR In_2O_3 II AND Tl_2O_3 II

	In_2O_3 II			Tl_2O_3 II		
Index	d_o	d_c	I_o	d_o	d_c	I_o
012	3.973	3.975	42	4.132	4.134	32
				3.446		2
				3.291		2
				3.176		2
104	2.883	2.883	100	2.976	2.976	90
110	2.743	2.743	96	2.874	2.873	100
006	2.418	2.418	16	2.475	2.475	4
113	2.387	2.386	16	2.484	2.485	4
202	2.258	2.258	16	2.359	2.359	2
024	1.987	1.987	70	2.067	2.067	80
116	1.814	1.814	60	1.875	1.875	30
122	1.743	1.743	8	1.823	1.823	5
018	1.694	1.694	22	1.739	1.739	22
214	1.609	1.609	38	1.678	1.678	60
030	1.584	1.584	34	1.659	1.659	50
208	1.441	1.442	6	1.488	1.488	12
1,0,10		1.388		1.423	1.423	8
220	1.371	1.372	17	1.437	1.437	20
036	1.325	1.325	8			
312	1.296	1.297	2			
128	1.276	1.276	10	1.321	1.321	10
134		1.239		1.294	1.294	14

eter were also grown in a NaOH flux using the method of Remeika and Marezio.[14] Crystals doped with Sn^{4+} were grown by introducing several per cent $SnCl_4$. The Sn^{4+}-doped (about 2 mol %) crystals exhibited a room-temperature resistivity of 10^{-4} ohm cm with a positive temperature dependence which may be compared to 10^{-3} ohm cm for undoped In_2O_3 (see Table II). Similar behavior has been noted for Sb^{5+}-doped SnO_2 crystals.[15]

Tl_2O_3.—Hoekstra[16] reported synthesis of a rhombohedral form of Tl_2O_3 at high pressures. Our experiments confirm this result. At temperatures above 500–600° and a pressure of 65 kbars fine black crystals were formed. Powder diffraction patterns indicated the corundum structure. Black crystals 0.5 mm long were grown by slow cooling to 300°. Oxygen analysis performed on Tl_2O_3 II by a catalytic fusion method showed 10.6% O and compares well with the theoretical oxygen content of 10.51%. However, the method is not sensitive enough to detect small deviations from stoichiometry.

Transformation to Tl_2O_3 I is believed to occur at 200–250°. A dta exotherm appeared at 250° and observation under a hot-stage microscope showed disintegration at 210°.

Ga_2O_3–Fe_2O_3.—At normal pressures this system is characterized by an intermediate compound, orthorhombic $Ga_xFe_{2-x}O_3$.[17] We find, in agreement with Marezio and Remeika,[10] that at pressures above 23 kbars at 1200° a complete solid-solution series is formed. The intermediates have the corundum structure and are reddish brown, and crystals have a columnar habit. Cell dimensions for the series are plotted in Figure 1. No ordering lines which might have been expected for the ilmenite structure were found.

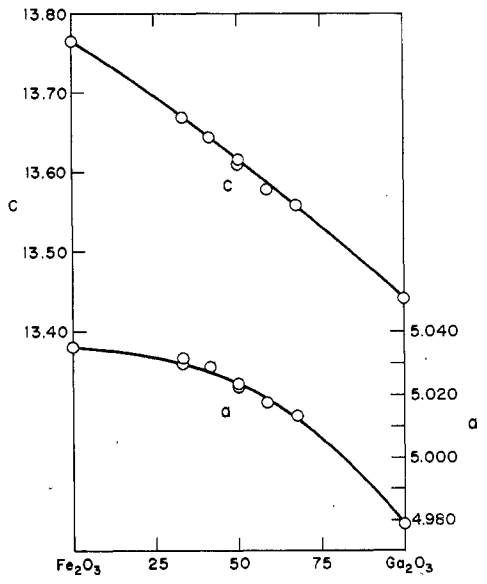

Figure 1.—Cell dimensions for the Fe_2O_3–Ga_2O_3 system quenched from 65 kbars.

In_2O_3–Fe_2O_3.—Schneider, *et al.*,[18] and Geller, *et al.*,[19]

(14) J. P. Remeika and M. Marezio, *Appl. Phys. Letters*, **8**, 87 (1966).
(15) D. F. Morgan and D. A. Wright, *Brit. J. Appl. Phys.*, **17**, 337 (1966).
(16) H. R. Hoekstra, personal communication at 150th Annual Meeting of the American Chemical Society, Atlantic City, N. J., Sept 17, 1965.
(17) J. P. Remeika, *J. Appl. Phys.*, **31**, 263S (1960).
(18) S. J. Schneider, R. S. Roth, and J. L. Waring, *J. Res. Natl. Bur. Std.*, **65A**, 345 (1961).
(19) S. Geller, H. J. Williams, and R. C. Sherwood, *J. Chem. Phys.*, **35**, 1908 (1961).

reported a limited solid solubility of In_2O_3 in Fe_2O_3 at normal pressures. At 65 kbars and 1200° solid solubility over the entire range occurred. As in the Ga_2O_3–Fe_2O_3 system no indication of ordering was detected. Cell dimensions are plotted in Figure 2. The products

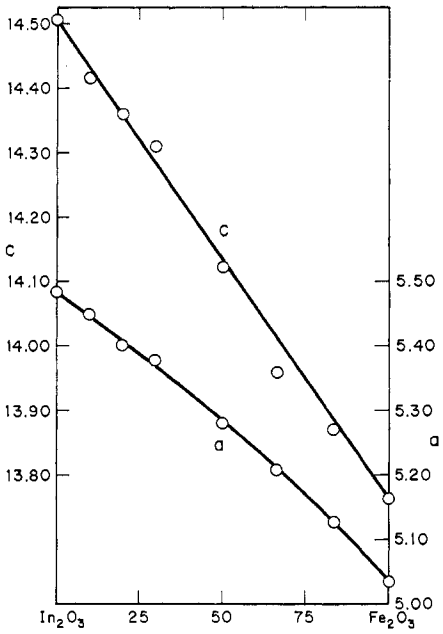

Figure 2.—Cell dimensions for the In_2O_3–Fe_2O_3 system quenched from 65 kbars.

were microcrystalline and reddish brown. The corundum phase with the $InFeO_3$ composition did not revert to a two-phase system after heating to 1000° in air.

In_2O_3–Sc_2O_3.—At normal pressures the system is characterized by complete solid solution having the C structure.[18] At 150 kbars and 1000° Sc_2O_3 has the B structure.[20] At 65 kbars and 1400° we find solubility of Sc_2O_3 in In_2O_3 II up to approximately the 1:1 composition. A 6:4 Sc_2O_3–In_2O_3 mixture produced transparent crystals 0.5 mm in diameter. X-Ray analysis of the entire sample showed a corundum phase and a trace of Sc_2O_3. Table II gives the cell dimensions of the 1:1 composition. Parameters for the composition $In_{1.5}Sc_{0.5}O_3$ are $a = 5.445 \pm 5$ Å and $c = 14.47 \pm 2$ Å.

Heating at 950° in air caused crystals of $InScO_3$ to disintegrate. X-Ray powder patterns of the product showed the presence of the C solid-solution phase.

Tl_2O_3–In_2O_3.—No reference to work on this system could be found in the literature. At 65 kbars and 800° the 1:1 composition has the corundum structure. At lower temperatures a solid solution of the C structure with $a = 10.33 \pm 1$ Å was found. Since the 1:1 composition has the corundum structure at high pressure, the system probably shows complete solid solubility. Observation under a hot-stage microscope showed condensation of vapors at 850°. The product was a C solid solution with $a = 10.3$ Å.

Effects of Pressure on Other R_2O_3 Oxides

Lu_2O_3 and Tm_2O_3 at 65 kbars and 1400° transformed to B structure, as shown by Hoekstra.[5] Mn_2O_3, after heating at 1300° under 65 kbars pressure in these experiments, was characterized by an X-ray diffraction pattern that was first thought to be of the C type but which is apparently a distortion of that structure.[21,22] Y_2O_3 and Sc_2O_3, heated at 89 kbars and 1300°, had the B and C structures, respectively.

X-Ray Studies of In_2O_3 II and Tl_2O_3 II

After the crystals of In_2O_3 II and Tl_2O_3 II were made in the present investigation, work was initiated on refinements of these structures. Independently, Christensen, *et al.*,[4] have refined the structure of In_2O_3 II. However, since our refinement results are somewhat different from those of Christensen, *et al.*, a brief review of our structure investigations is included here.

Refinement of In_2O_3 II.—Table I gives the cell parameters of In_2O_3 II determined from a least-squares refinement of Guinier-photograph data. A single crystal was selected from the same sample and ground to a sphere of radius 0.0033 cm. Other data are formula weight = 277.64, D_m = 7.31 g/cm³ (displacement method using bromoform), $Z = 6$, $D_x = 7.311$ g/cm³, $\mu = 179$ cm^{-1} (Mo Kα), and space group R3c-C_{3v}^6 or R$\bar{3}$c-D_{3d}^6. (Absences, from precession photographs: hkl, $-h + k + l \neq 3n$, $hh\bar{l}$, $l \neq 2n$.) Space group R$\bar{3}$c was adopted by analogy to other corundum structures.

Intensities were measured using a Picker automatic diffractometer, Nb-filtered Mo Kα radiation, and a scintillation detector. Reflections were scanned at 0.5°/min through an angle of 1.6° plus the $\alpha_1 - \alpha_2$ separation. Background was measured for 20 sec at the extremes of each scan. A total of 210 reflections was measured in a volume equivalent to one-sixth of reciprocal space out to a sin θ equivalent to the Cu Kα radiation limit. Combining equivalent reflections left a set of 100 nonequivalent reflections. Corrections for absorption were made by the method of Wuensch and Prewitt,[23] and at the same time the Zachariasen[24] secondary extinction parameter β was computed for each reflection. This was later used to correct the observed structure factors using

$$F_{cor} = F_o(1 + \beta C I_o)$$

where C is a least-squares variable and I_o is the integrated intensity.

σ's[25,26] for each reflection were computed using

$$\sigma_{F_o} = (LpT)^{-1/2}[(I + \sigma_I)^{1/2} - I^{1/2}]$$

where L, p, and T are the Lorentz, polarization, and transmission factors, respectively, and

$$\sigma_I = \left[E + \left(\frac{T_E}{2T_B}\right)^2 (B_1 + B_2) + \epsilon^2 I^2\right]^{1/2}$$

(20) A. F. Reid and A. E. Ringwood, see ref 6.
(21) S. Geller, J. A. Cape, R. W. Grant, and G. P. Espinosa, *Phys. Letters*, **24A**, 369 (1967).
(22) R. Norrestam, *Acta Chem. Scand.*, **21**, 2871 (1967).
(23) B. J. Wuensch and C. T. Prewitt, *Z. Krist.*, **122**, 24 (1965).
(24) W. H. Zachariasen, *Acta Cryst.*, **16**, 1139 (1963).
(25) D. E. Williams and R. E. Rundle, *J. Am. Chem. Soc.*, **86**, 1660 (1964).
(26) R. D. Ellison and H. A. Levy, *Acta Cryst.*, **19**, 260 (1965).

Here E is the total count including background, T_E and T_B are the peak and background times, B_1 and B_2 are background counts, and ϵ, set in this case to 0.03, is a factor put in to account for fluctuations in X-ray beam intensity and other uncertainties.

Parameters were refined by least squares using a full-matrix program[27] which minimizes $\Sigma w||F_o| - |F_c||^2$, where weights, w, were the reciprocal squares of corresponding σ's. The atomic scattering factor curve for In^{3+} was taken from Cromer and Waber[28] and for O^{2-} from Tokonami.[29] The real and imaginary anomalous dispersion corrections for In were from Cromer.[30] After several cycles of atom coordinate and isotropic temperature factor refinement, R $(=\Sigma||F_o| - |F_c||/\Sigma|F_o|)$ was 0.05. Then anisotropic temperature factors and, finally, the secondary extinction parameter C were varied resulting in a final R of 0.022 for all reflections and 0.018 for 94 observed reflections included in the least-squares matrix. The weighted R is 0.030 and the standard deviation of an observation of unit weight is 1.19. The parameter C is 0.21 (6) $\times 10^{-5}$.

Final observed and calculated structure factors are listed in Table IV, refined parameters are given in Table V, and bond distances and angles are given in Table VI along with the equivalent distances and angles from other refinements of compounds with the corundum structure. Figure 3 is a schematic drawing of the corundum structure. In Table VI and Figure 3 the designations of atom positions are those of Newnham and de Haan.[7]

TABLE IV

OBSERVED AND CALCULATED STRUCTURE FACTORS[a]

H	K	L	FOB	FCA	H	K	L	FOB	FCA	H	K	L	FOB	FCA	H	K	L	FOB	FCA
3	0	0	4366	4405	5	3	3	114	27*	5	1	7	189	208	3	1	11	93	59*
6	0	0	2321	2310	1	4	3	248	239	3	2	7	154	157	1	2	11	148	130
1	1	0	4218	4179	1	0	4	4345	4159	1	3	7	117	103*	2	3	11	157	132
4	1	0	2683	2662	4	0	4	2435	2442	2	4	7	162	156	0	0	12	275	271
2	2	0	3128	3225	2	1	4	3458	3545	2	0	8	2100	2138	3	0	12	317	305
3	3	0	2663	2701	5	1	4	2150	2162	5	0	8	1397	1351	1	1	12	941	891
2	1	1	279	275	0	2	4	4007	4052	0	1	8	2567	2585	4	1	12	593	597
5	1	1	213	224	3	2	4	2661	2686	3	1	8	1903	1914	2	2	12	748	721
3	2	1	186	184	1	3	4	2719	2762	1	2	8	1998	2020	0	3	12	313	308
1	3	1	136	118	2	4	4	2165	2167	4	2	8	1369	1354	1	4	12	583	593
4	3	1	115	23*	0	5	4	2356	2392	2	3	8	1476	1483	2	1	13	146	127
2	4	1	184	164	3	1	5	101	94*	0	4	8	1883	1910	3	2	13	142	120
2	0	2	769	767	1	2	5	232	220	1	5	8	1256	1221	1	3	13	110	78*
5	0	2	458	440	4	2	5	140	146	1	1	9	460	478	2	0	14	2663	2644
0	1	2	1456	1313	2	3	5	151	169	4	1	9	178	200	0	1	14	2685	2685
3	1	2	871	892	1	5	5	203	211	2	2	9	294	278	3	1	14	2130	2148
1	2	2	782	797	0	0	6	1823	1770	3	3	9	135	23	1	2	14	2470	2483
4	2	2	527	508	3	0	6	1614	1623	1	4	9	190	195	0	4	14	1979	1975
2	3	2	487	486	1	1	6	2917	2911	1	0	10	3240	3223	1	1	15	276	269
0	4	2	938	958	4	1	6	1708	1717	4	0	10	2437	2447	2	2	15	203	195
3	4	2	665	674	2	2	6	2118	2146	2	1	10	2619	2641	1	0	16	458	455
1	5	2	399	392	0	3	6	1614	1626	0	2	10	2760	2773	2	1	16	496	487
1	1	3	816	875	3	3	6	1281	1251	3	2	10	2025	2006	0	2	16	567	554
4	1	3	240	242	1	4	6	1692	1715	1	3	10	2482	2483	0	0	18	2171	2277
2	2	3	436	384	2	1	7	196	201	0	5	10	1837	1825	1	1	18	1786	1793

[a] FOB is $10F_o$ and FCA is $10F_c$. "Unobserved" reflections are marked with an asterisk.

A comparison of the In_2O_3 II bond distances from Table VI with those of Christensen, *et al.*,[4] shows differences ranging from 0.01 to 0.07 Å. However, the Christensen values were obtained using relatively imprecise data resulting in stated errors of 0.05 Å for the In–O distances. The average In–O distances are similar, however, with 2.17 Å from Christensen *vs.* 2.187 Å from Table VI. Marezio[31] has reported 2.18 Å for the average In–O distance in In_2O_3 I.

(27) C. T. Prewitt, unpublished computer program, 1966.
(28) D. T. Cromer and J. T. Waber, *Acta Cryst.*, **18**, 104 (1965).
(29) M. Tokonami, *ibid.*, **19**, 486 (1965).
(30) D. T. Cromer, *ibid.*, **18**, 17 (1965).
(31) M. Marezio, *ibid.*, **20**, 723 (1966).

TABLE V

REFINEMENT RESULTS FOR In_2O_3 II[a]

	In	O
x	0	0.2980 (5)
y	0	0
z	0.35731 (2)	1/4
B_{11}, Å^2	0.36 (3)	0.05 (8)
B_{22}, Å^2	0.36 (3)	0.09 (9)
B_{33}, Å^2	0.41 (3)	0.51 (8)
B_{12}, Å^2	0.18	0.05
B_{13}, Å^2	0	0.11 (6)
B_{23}, Å^2	0	0.22
Equivalent isotropic B	0.38	0.22

[a] The expression $\exp[-(h^2\beta_{11} + k^2\beta_{22} + l^2\beta_{33} + 2hk\beta_{12} + 2hl\beta_{13} + 2kl\beta_{23})]$ was used in calculating structure factors. For this table the β_{ij} have been converted to B_{ij} using $B_{ij} = 4\beta_{ij}/b_ib_j$ where b_i are the reciprocal cell parameters. For In, $B_{11} = B_{22} = 2B_{12}$; $B_{13} = B_{23} = 0$. For O, $B_{22} = 2B_{12}$; $2B_{13} = B_{23}$.

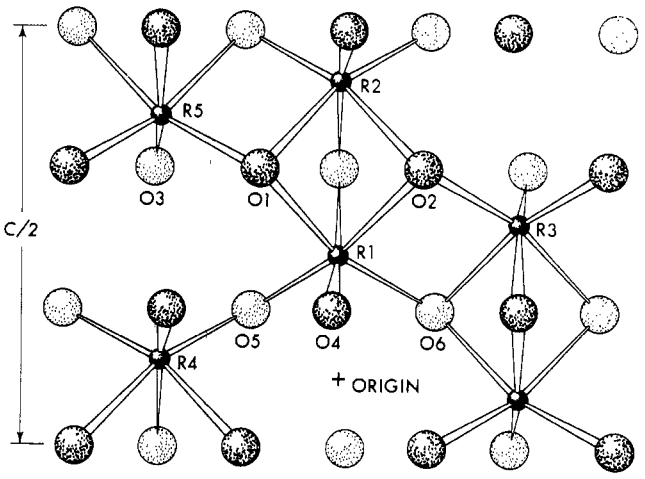

Figure 3.—The corundum structure viewed along an a axis of the hexagonal cell (after Newnham and de Haan[7]).

The equivalent isotropic temperature factor for oxygen is rather small (0.22), but the one for In (0.38) is nearly identical with that obtained by Marezio for In_2O_3I.[31] Additional refinement cycles were tried using "neutral" scattering factor curves which resulted in higher equivalent B's for In (0.49) and O (0.26). The z coordinate for In was unchanged and the x coordinate for O changed less than 1σ. Variations of In–O distances were on the order of ± 0.001 Å. The anisotropic temperature coefficients indicate that In thermal vibrations are nearly isotropic whereas O is markedly anisotropic and has its major axis vibrating normal to a at about 30° to c. This direction approximately bisects the largest angles subtended at oxygen, R(1)–O(1)–R(5).

Tl_2O_3 II.—Attempts were made to obtain X-ray data for Tl_2O_3 II using either single-crystal or powder X-ray techniques. However, the crystals taken from the high-pressure runs were of poor quality and no reliable single-crystal intensity data could be obtained. Furthermore, the limited crystalline material that was available was very platy, exhibiting faces which were predominantly (012). Because of marked preferred

TABLE VI

COMPARISON OF INTERATOMIC DISTANCES AND BOND ANGLES IN REFINED CORUNDUM STRUCTURES

	Al_2O_3[a]	Cr_2O_3[a]	Ga_2O_3[b]	V_2O_3[a]	Fe_2O_3[c]	Ti_2O_3[a]	In_2O_3[d]
Distance	Å						
R(1)–O(1)	1.97	2.02	2.077	2.06	2.116	2.08	2.256 ± 3
R(1)–O(5)	1.86	1.97	1.921	1.96	1.945	2.01	2.118 ± 2
R(1)–R(2)	2.65	2.65	2.835	2.70	2.900	2.59	3.114 ± 1
R(1)–R(3)	2.79	2.89	2.938	2.88	2.971	2.99	3.243 ± 1
R(1)–R(4)	3.22	3.43	3.313	3.47	3.364	3.56	3.606 ± 1
R(1)–R(5)	3.50	3.65	3.645	3.69	3.706	3.74	3.986 ± 1
O(1)–O(2)	2.52	2.63	2.630	2.70	2.669	2.83	2.827 ± 7
O(1)–O(3)	2.87	2.99	3.007	2.94	3.035	3.05	3.351 ± 4
O(1)–O(4)	2.62	2.74	2.716	2.81	2.775	2.80	2.938 ± 1
O(1)–O(5)	2.73	2.85	2.833	2.89	2.888	2.88	3.097 ± 1
Angle	Deg						
R(1)–O(1)–R(2)	84.6	82.3	86.1	81.7	86.6	76.9	87.29 ± 14
R(1)–O(2)–R(3)	93.6	93.1	94.5	91.4	94.0	93.7	95.68 ± 3
R(1)–O(5)–R(4)	120.3	121.4	119.1	124.4	119.7	124.2	116.71 ± 18
R(1)–O(1)–R(5)	132.3	133.1	131.5	132.9	131.7	132.0	131.33 ± 5
O(1)–R(1)–O(2)	79.7	81.4	78.6	81.9	78.2	85.4	77.61 ± 11
O(1)–R(1)–O(5)	86.4	86.9	85.5	88.6	86.1	86.3	90.11 ± 8
O(5)–R(1)–O(6)	101.1	99.0	103.0	97.0	102.6	98.4	104.59 ± 3
O(1)–R(1)–O(6)	164.3	167.0	162.0	169.1	162.4	170.5	159.92 ± 11
O(1)–R(1)–O(4)							84.32 ± 3
Parameter							
x(O)	0.306	0.306	0.3049	0.315	0.3059	0.317	0.2980
z(R)	0.3520	0.3475	0.3554	0.3463	0.3553	0.3450	0.3573

[a] Reference 7. [b] Reference 10. [c] Reference 9. [d] This work.

orientation of the powder samples, attempts at refining the powder data were also unsuccessful.

A possibility exists that Tl_2O_3 II does not have the corundum structure but a distorted one that gives rise to a similar diffraction pattern. Some upper level precession photographs do not show threefold symmetry, but it is not clear whether this is due to a truly lower symmetry or to poor crystals. Careful examination of powder photographs reveals three faint lines not indexable (see Table III) on the basis of the unit cell listed in Table I. Furthermore, Tl_2O_3 II lines are broader than those of In_2O_3 II; however, no split lines can be seen.

Discussion

The C Rare Earth Oxide–Corundum Transition.—It is apparent from these experiments that the C rare earth oxide–corundum transition is common to two compounds and several solid solutions. The $In_{2-x}Fe_xO_3$ system at atmospheric pressure exhibits only a partial solid solubility, with the C structure occurring in the compositional range $0 \leq x \leq 0.87$ and the corundum structure at values of x only slightly less than 2. However, at elevated pressure the system forms a complete solid solution series having the corundum structure. In the $In_{2-x}Sc_xO_3$ series at atmospheric pressure there is a complete solid solution of end members with C structure, while at 65 kbars solid solution occurs only to $x = 1$. The structure of the high-pressure series up to $x = 1$ is that of corundum and at higher x a two-phase mixture results.

It is helpful to look at the effects of pressure on the simple oxides Mn_2O_3, Sc_2O_3, Lu_2O_3, Tm_2O_3, and Y_2O_3. These oxides are isotypic with In_2O_3 I and are characterized by cations whose radii are smaller or similar in size to the radii of In^{3+} and Tl^{3+}.[11] Yet, none of these oxides, with the possible exception of Mn_2O_3, appears to assume the corundum structure at high pressure. Although it is dangerous to draw conclusions about the phase present at high pressure from identification of the quenched product, the presence of large crystals suggests that rapid reconstructive transformation did not take place. Thus, because transparent crystals of C type Sc_2O_3 and B type Lu_2O_3, Tm_2O_3, and Y_2O_3 were recovered from the quenching experiments, it seems likely that these structure types are the stable ones at 65 kbars. In the case of Mn_2O_3 the product was finely powdered and apparently possessed the distorted bixbyite structure. In view of the powder form of the product it is possible that a different structure was stable at high pressure. It is apparent that ionic size, although traditionally the criterion for classifying the rare earth oxides, is not the only factor in the determination of which structure will occur at high pressure.

On the basis of cation coordination and density the order of stability of the phases with increasing pressure should be: C → corundum → B. The coordination of the cations in the B structure is closer to seven than six and the densities of the B phases are about 8% greater than those of the equivalent C phases. The density of In_2O_3 II is only about 2.5% larger than In_2O_3 I. The sequence of phases mentioned above has not yet been observed for any oxide. The apparent absence of a corundum phase for Sc_2O_3, Lu_2O_3, Tm_2O_3, and Y_2O_3 can be rationalized by considering electronegativity differences in relation to the available structure.

In both the In_2O_3 I and In_2O_3 II structures the cations are six-coordinated and the anions are four-coordinated. The cation–anion distances are nearly identical in the

two structures. The densities are similar and the difference that does exist results from better packing of the anion layers in the corundum (In_2O_3 II) modification. The anion layers in corundum are somewhat distorted from a close-packed hexagonal arrangement (ABAB). However, in the C structure in In_2O_3 I the anion layers, which can be considered as being in a close-packed cubic (ABCABC) arrangement with anion vacancies, are considerably more distorted. At high pressure, stabilization of the corundum phase presumably is caused by the small increase of density (2.5%) resulting from the formation of less distorted, vacancy-free anion layers. The transformation also results in a change of coordination polyhedra. Although cations in both structures are six-coordinated, those of In_2O_3 II are in a rather regular octahedron, while those of In_2O_3 I are coordinated by O at six of the eight corners of a cube. Significantly, oxygen in both structures is in essentially tetrahedral coordination by cations.

While there are important differences between the C and corundum structures as noted above, they are considerably more similar to each other than either is to the B structure adopted at high pressure by Sc_2O_3, Lu_2O_3, Tm_2O_3, and Y_2O_3. The latter structure[32] contains two crystallographically distinct cations each coordinated by oxygen atoms arranged in monocapped trigonal prisms and a third cation position in octahedral coordination. The capping oxygens on the rectangular faces of the trigonal prism are farther away than are the other oxygens. However, if the cation coordinations are taken to be seven, seven, and six, then the coordination numbers for five different oxygen ions in the structure are four, four, four, five, and six. It is this higher average coordination in the B structure that perhaps affords a clue to the high-pressure stabilization of In_2O_3 and Tl_2O_3 in corundum rather than in the denser B form. The oxides of indium and thallium are expected to be considerably more covalent than those of scandium, yttrium, and the rare earths. This is clearly demonstrated in tables of electronegativities.[33,34] For oxide compositions with high degrees of covalence the more favorable structures are those in which oxygen can use sp^3 hybrid orbitals in bonding to each neighboring cation. In the cases under consideration here, tetrahedral coordination of oxygen as in the corundum and C structures would permit a higher degree of covalence relative to the five- and six-coordinated oxygens in the B and A structures. The latter would be expected to be more stable for compounds with higher ionic character such as Sc_2O_3, Lu_2O_3, Tm_2O_3, and Y_2O_3. A second effect of covalence is the reduction of effective charge at the ion centers. Thus, the effective cationic charge in In_2O_3 and Tl_2O_3 is probably considerably less than in the rare earth oxides. This situation greatly reduces electrostatic repulsion between cation near neighbors and would provide a more favorable condition for octahedral face sharing that occurs in the corundum structure. The relatively greater repulsion between near cation neighbors in the RE oxides probably explains the absence of the corundum phase in these oxides.

In order to determine whether there is any significant difference in the electrostatic energies of the In_2O_3 I and In_2O_3 II structures, we calculated the Madelung constants for each using the refined atom coordinates for In_2O_3 I from Marezio[31] and the coordinates for In_2O_3 II from Table V. The calculations were made using Baur's program MANIOC[35] assuming completely ionized atoms. The program was tested for the C structure by repeating the Mertens and Zemann[36] calculation for Y_2O_3. Their value of the Madelung constant using the parameters from a least-squares refinement of the Y_2O_3 structure is 25.087_9 as compared to our value of 25.087_1. The Madelung constants for In_2O_3 I and In_2O_3 II are 24.498_4 and 24.333_5, respectively. These numbers correspond to Madelung or electrostatic energies of -3822 and -3816 kcal/mol per formula unit. Although one should probably not read too much significance into these numbers because other contributions to the total energy have been ignored, it is evident that since the energies are close to each other, the structures are electrostatically similar. If the numbers are significant, In_2O_3 I is the stable phase under ambient conditions, as is observed.

Correlation of Crystallographic Parameters with Electron Configuration

The availability of crystallographic data for In_2O_3 II and Tl_2O_3 II with unit cells considerably larger than those of other R_2O_3 compositions having the corundum structure now permits a view of the general crystal chemistry of the corundum phases in a much broader context. For example, a definite radius dependence of the c/a ratio of corundum structures is observed. The empirical equation for this dependence is $c/a = 2.73 - 0.33(r_R - r_{Al})$. Thus, the addition of $0.33 \cdot (r_R - r_{Al})$ to all observed c/a ratios provides a set of normalized values which do not reflect the radius dependence and which permit an assessment of electron configuration on the c/a ratio (Figure 4).

A more complete correlation of interatomic distances in corundum can also now be made; *e.g.*, see Figure 5 and Table VI. Goodenough has proposed that there are metal–metal bonds across the shared octahedral faces in Cr_2O_3, V_2O_3, and Ti_2O_3.[37,38] The anomalously short R(1)–R(2) distances indicated by Figure 5 for these oxides give strong support to this proposal. Although the R(1)–R(2) distance in Al_2O_3 is short in absolute terms, Figure 5 indicates that this distance is not *anomalously* short and neither is the R(1)–R(2) distance in In_2O_3 II *anomalously* long.

The corundum structure is notable in that it contains RO_6 octahedra that share one face and three

(32) D. T. Cromer, *J. Phys. Chem.*, **61**, 753 (1957).
(33) A. L. Allred, *J. Inorg. Nucl. Chem.*, **17**, 215 (1961).
(34) L. Pauling, "The Nature of the Chemical Bond," Cornell University Press, Ithaca, N. Y., 1960, p 93.
(35) W. H. Baur, *Acta Cryst.*, **19**, 909 (1965).
(36) H.-E. v. Mertens and J. Zemann, *ibid.*, **21**, 467 (1966).
(37) J. B. Goodenough, "Magnetism and the Chemical Bond," Interscience Division, John Wiley & Sons, Inc., New York, N. Y., 1963.
(38) J. B. Goodenough, *Bull. Soc. Chim. France*, **4**, 1200 (1965).

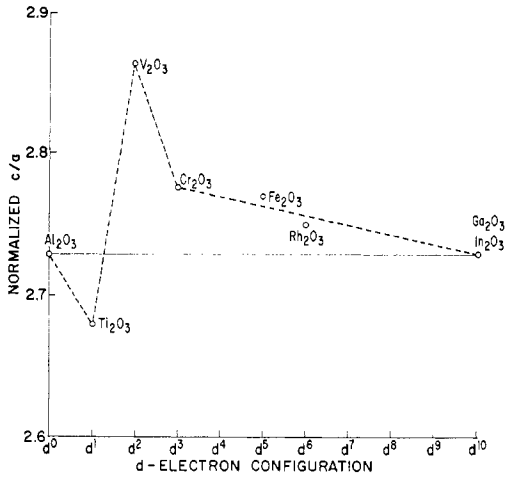

Figure 4.—Normalized c/a as a function of d-electron configuration. See text for definition of normalized c/a.

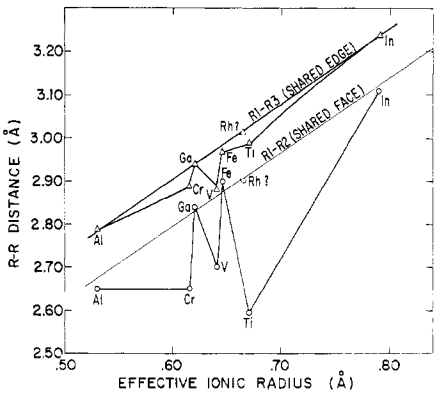

Figure 5.—Metal–metal distances *vs.* effective ionic radius.

edges with other octahedra. The oxygen ions, each of which is coordinated by four cations, are in an approximately close-packed hexagonal arrangement. In an ideal close-packed hexagonal arrangement the coordinates of R(2) and O(1) of Figure 3 would be 0, 0, $^1/_3$ and $^1/_3$, 0, $^1/_4$, respectively. In all compounds with the corundum structure the cations across the shared octahedral face are displaced away from each other and the oxygens in the shared face are displaced toward each other with respect to the ideal coordinates. These displacements are less for those compounds which form metal–metal bonds across the face (Table VI). The cell volumes for corundums are nearly proportional to the cubes of the cation radii[11] (Figure 6) in spite of extreme variations in the interatomic distances with ionic size.

Strong electrostatic repulsive forces exist between the cations across both the shared face and shared edges in the corundum structure. Although increases in the c axes reflect increased metal–metal face distances, changes in the cation z parameters reduce the total change in c which would be required to accommodate the increased repulsion. However, since the metal–metal edge distances are less sensitive to changes in the cation z parameter, the repulsion across edges is more strongly reflected in increases in a. Consequently, the c/a ratios for corundums are all considerably smaller than the ideal value of 2.82 for hexagonal close packing with the exception of V_2O_3.

Goodenough[37,38] and Adler, *et al.*,[39,40] have considered metal–metal bonding and the electrical properties of transition metal oxides in detail. The bonding situation in Ti_2O_3 is simplest since there is only one electron per cation. The correlations of this paper strongly support Goodenough's proposal of a metal–metal bond at room temperature. An alternate view that Ti_2O_3 is simply antiferromagnetic has apparently been ruled out by a recent neutron diffraction study.[41]

In V_2O_3 an additional electron per cation is available. This electron might be used either for the formation of a double bond across the face or for metal–metal bonding across the shared octahedral edges. From Figure 5 it is evident that the latter has likely happened. The metallic behavior of V_2O_3 at room temperature further indicates that the interactions across edges are significant because the interactions across the faces are finite and could not lead to metallic conductivity. Goodenough has suggested that below the metal to semiconductor transition in V_2O_3 at 150°K the metal atoms are paired across edges as well as faces.[37] However, since the structure of the low-temperature form is not known, it is difficult to speculate about the bonding in this form. Figure 5 indicates that metal–metal bonding across edges is not present in either Cr_2O_3 or Fe_2O_3. This conclusion is further supported by the physical properties of these compounds (Table I).

The breakdown of metal–metal bonding on proceeding from left to right across the transition series occurs before the number of electrons is sufficient to suggest that they would have antibonding character with respect to metal–metal interactions. Therefore, the disappearance of metal–metal bonding apparently results from contracting d orbitals. A very analogous situation has been observed for the transition metal dioxides with the rutile structure.[42] Since the metal–metal distances across the faces are shorter than those across the edges, it is expected (and observed) that the metal–metal bonding across the edges would break down before that across the faces.

The c/a *vs.* electron configuration plot in Figure 4 is readily rationalized if it is realized that the metal–metal distances across the shared octahedral face affect the cation z parameter as well as the size of the c axis and that metal–metal distances across the shared edge primarily affect the size of the a axis. Thus, in Ti_2O_3 where there is metal–metal bonding only along c, there is a low c/a ratio (Figure 4), but in V_2O_3 the short metal–metal distance along c is obtained with a high c/a ratio. The high c/a ratio in V_2O_3 is the result of the metal–metal bonding across the octahedral edges. It might be expected that Cr_2O_3 would be similar to

(39) D. Adler, J. Feinleib, H. Brooks, and W. Paul, *Phys. Rev.*, **155**, 851 (1967).
(40) D. Adler, *Solid State Phys.*, **21**, 1 (1968).
(41) H. Kendrick, A. Arrott, and S. A. Werner, *J. Appl. Phys.*, **39**, 585 (1968).
(42) D. B. Rogers, R. D. Shannon, A. W. Sleight, and J. L. Gillson, *Inorg. Chem.*, **8**, 841 (1969).

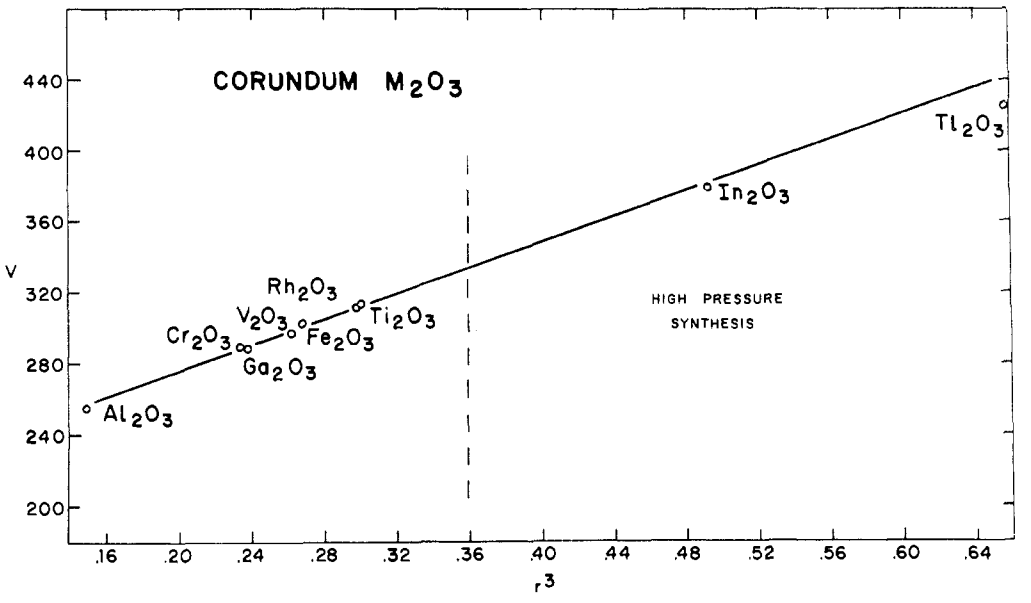

Figure 6.—Corundum unit cell volumes *vs.* effective cation volume (r_c^3).

Ti_2O_3 in the c/a ratio since both have metal–metal bonding across the face but not across the edges. However, Cr^{3+} has two more electrons than Ti^{3+}, and these are concentrated in the *ab* plane separating the oxygen layers and preventing them from contracting along *c*.

The behavior of the $(Ti_{1-x}V_x)_2O_3$ solid-solution series[43] from $x = 0.0$ to $x = 0.10$ is consistent with the metal–metal bonding scheme outlined above. The abrupt rise in the c/a ratio as Ti^{3+} is replaced by V^{3+} is the result of bonding across the edges. The decrease in *a* caused by this bonding is compensated by an increase in *c*.

All sets of R–O distances are consistent with the metal–metal bonding considerations. This is apparent when ions of similar size but different electron configurations (V^{3+} or Fe^{3+} and Cr^{3+} or Ga^{3+}) are compared. Metal–oxygen distances (R(1)–O(1)) are shorter and the distances R(1)–O(5) are longer in Ti_2O_3, V_2O_3, and Cr_2O_3 than distances that would be predicted only on the basis of changes in ionic size. Oxygen distances O(1)–O(2) in the shared face are larger with respect to ionic size in Ti_2O_3 and V_2O_3 than in the other structures, reflecting the short R(1)–R(2) distances. The oxygen distance in the shared edge (O(1)–O(4) or O(2)–O(6)) is anomalously large in only V_2O_3. The angles R(1)–O(1)–R(2) are smaller in Ti_2O_3, V_2O_3, and Cr_2O_3 than in the other corundum oxides, presumably because of the metal–metal bonding across the shared face. In fact, for each type of angle given in Table VI, the values for Ti_2O_3, V_2O_3, and Cr_2O_3 are nearly always either larger or smaller than for the other compositions.

Of the known simple oxide compounds with the corundum structure, only Rh_2O_3 and Tl_2O_3 II remain for structure refinement. There are problems with Tl_2O_3 II which were mentioned previously; however, a prediction of the atomic coordinates of Rh_2O_3 can be made based on Figures 5 and 6. In Figure 6, Rh_2O_3 is on the line, and the average Rh–O distance should be close to 2.05 Å. Since metal–metal bonding is not expected for Rh^{3+} ($4d^6$) and since Rh_2O_3 behaves normally in Figure 4, there is good reason to believe that Rh will fall very close to the lines in Figure 5. With this assumption, the Rh(1)–Rh(2) distance is 2.90 Å. This results in coordinates for Rh(2) of 0, 0, 0.355. Parameters of 0.305, 0, $1/4$ for O(1) give Rh(1)–O(1) and R(1)–O(4) distances of 2.13 and 1.97 Å and an average Rh–O distance of 2.05 Å.

Acknowledgments.—The authors are indebted to C. L. Hoover for performing the high-pressure experiments, to Dr. J. F. Whitney and Miss M. S. Licis for assistance in obtaining the X-ray data, and to J. L. Gillson for performing the resistivity measurements.

(43) T. Kawakubo, T. Yanagi, and S. Nomura, *J. Phys. Soc. Japan*, **15**, 2102 (1960).